RSC Advances

PAPER

Cite this: *RSC Adv.*, 2022, **12**, 15158

Effect of chloride ions on the corrosion behavior of carbon steel in an iron bacteria system

Ping Xu,* Meihui Zhao, † Xue Fu† and Chen Zhao

Reclaimed water used as circulating cooling water can effectively relieve water stress, but the corrosion problem in it is very prominent. In particular, Cl^- and iron bacteria (IB) are important influencing factors of corrosion behavior in a circulating water environment, and both of them often coexist in circulating water systems, so it is crucial to study their synergistic effects. This paper investigated the effect of Cl^- on the corrosion behavior of carbon steel in the IB system by use of weight loss measurements, electrochemistry and X-ray photoelectron spectroscopy (XPS). In the first 1–9 days of the experiment, the increase of Cl^- concentration led to an increase of corrosion rate and a decrease of anode potential and charge transfer resistance at the interface. The corrosion rate of the $4Cl_{IB}$ condition reached 0.45 mm a^{-1} in the 1st day, which was 1.47 and 1.15 times that of $3Cl_{IB}$ and $1Cl_{IB}$, and its anode potential was 22.6% and 33.8% lower than that of $3Cl_{IB}$ and $1Cl_{IB}$. This indicates that a higher concentration of Cl^- made the anodic reaction easier and the corrosion more severe. However, after 9 days, a decline in the corrosion rate was recorded at similarly high Cl^- concentrations. On the 15th day, the corrosion rates for $3Cl_{IB}$ and $4Cl_{IB}$ were 7.0% and 15.6% lower compared to the $1Cl_{IB}$ condition. At this stage, the anode potential and film resistance had increased significantly, to become the dominant factors controlling the corrosion reaction. On the 15th day, the β_a values of $1Cl_{IB}$, $3Cl_{IB}$ and $4Cl_{IB}$ were 1.2, 1.5 and 1.7 times higher than those of the 1st day, and the highest R_b value of 1592.1 Ω cm^2 was obtained for the $4Cl_{IB}$ condition, which was 1.9 times higher than that of R_{ct}. In the early stage of corrosion, the surface of the carbon steel was enriched in Cl^- due to their high concentration, and the Cl^- could easily destroy the developing corrosion product film and promote the generation of Fe^{2+}. At the same early stage, the growth of IB was enhanced, and the metabolism of IB was promoting local corrosion. However, in the later stage of corrosion, biofilms had an increasing effect on corrosion. A high concentration of Cl^- accelerated biofilm growth and densified the corrosion product layer which subsequently hindered the anodic reaction and thus inhibited corrosion.

Received 14th April 2022
Accepted 12th May 2022

DOI: 10.1039/d2ra02410a

rsc.li/rsc-advances

1 Introduction

Industrial circulating cooling water in China accounts for about 70% of industrial water consumption.[1] Recycling urban sewage water into industrial circulating cooling water can effectively alleviate the water shortage in China. However, the high content of organic matter in the reclaimed water provides conducive conditions for growth and adhesion of microorganisms, resulting in microbiological induced corrosion.[2] At the same time, the reclaimed water contains corrosive ions such as Cl^- and SO_4^{2-},[3] which also promote the corrosion of metal pipes and equipment, which can result in equipment failure and associated risks and can cause large economic losses.[4,5]

Many scholars have studied the corrosion mechanism of corrosive ions and microorganisms in reclaimed water. Cl^- ions are one of the ions that have the greatest impact on corrosion.[6–8] They have a small radius, strongly adsorb and easily penetrate the passivation layer aggravating metal corrosion. In the circulating water systems, the increase of Cl^- concentration can accelerate the uniform corrosion of carbon steel pipes and pitting corrosion of stainless-steel pipes.[9,10] Corrosion can also be aggravated by the presence of certain types of bacteria. Iron bacteria (IB) are one of the main corrosion inducing microorganisms, including iron-oxidizing bacteria (IOB) and iron-reducing bacteria (IRB). IOB can oxidize Fe^{2+} to form $Fe(OH)_3$ precipitates. These precipitates cover the tube wall to form small anode points that act as galvanic cells with a large area where oxygen exists, causing local corrosion.[11] On the other hand, IRB can reduce the insoluble Fe^{3+} precipitates to soluble Fe^{2+}, leading to the destruction of the passivation film, thereby aggravating the corrosion.[12] It has also been suggested that Fe^{2+} formed by the metabolism of IRB can form an ionic layer on the

Beijing University of Civil Engineering and Architecture, Beijing, 100044, China. E-mail: xuping@bucea.edu.cn

† These authors contributed to the work equally and should be regarded as co-second authors.

metal surface, which inhibits the attachment of dissolved oxygen and at the same time inhibits the dissolution and precipitation of anode iron, thus inhibiting corrosion.[13,14] Changes in Cl^- concentration can affect microbial growth, thereby altering the corrosion process.[15] Some studies have found that there is an optimal concentration of Cl^- that can promote the growth of sulfate reducing bacteria (SRB). Very low Cl^- concentration was found to have little effect on the corrosion behavior of SRB, however, when the concentration of Cl^- increased to 5–30 g L^{-1}, the salinity increased, which promoted the growth and attachment of SRB enhancing corrosion.[16,17] The concentration of Cl^- over 30 g L^{-1} was found to inhibit the growth of SRB and reduces corrosion.[17,18] Some studies suggest that the sulfide produced by the corrosion of SRB promoted the corrosion,[19] while other studies suggest that the synergistic effect of Cl^- and SRB caused pitting corrosion and accelerated the corrosion process.[17] Excessive Cl^- concentration will inhibit the diffusion of dissolved oxygen and SRB adhesion, resulting in a decrease in the corrosion rate.[18]

At present, the effect of Cl^- on the corrosion behavior of the SRB system is relatively clear, but it's effect on the corrosion behavior of IB is uncertain. Most of the existing research on the behavior of IB is based on the analysis of experiments done for a limited amount of time. Therefore, this study investigated the effect of Cl^- on the corrosion behavior of IB systems over the entire experimental duration. The corrosion process was analyzed by measuring corrosion weight loss and performing electrochemical tests. The components of corrosion products were analyzed by X-ray energy spectrometry. In addition, the amount of Cl^- and IB in suspended and attached states was also detected and measured.

2 Experimental

2.1 Materials

The national type I carbon steel coupon (50 mm × 25 mm × 2 mm) were prepared for dynamic testing. The elemental composition of the coupon was 99.421% Fe, 0.29% Mn, 0.17% Si, 0.095% C, 0.012% P and 0.012% S. Before the experiment, the coupons were soaked in acetone for 5 s to remove the surface grease, and then wiped with medical absorbent cotton and dried on a filter paper. The dried coupons were then rinsed with distilled water, soaked in absolute ethanol for 1 min and dried as before. The coupons were then wrapped with a filter paper, put in a desiccator for 1 day and weighed. They were sterilized under UV light for 30 minutes before use.

A 1 cm^2 carbon steel electrodes were prepared for electrochemical testing. This was done by mounting a piece of carbon steel in epoxy resin and leaving 1 cm^2 surface exposed to work as the electrode. Before use, the samples were polished step by step using a 180#–2000# abrasive paper, polished with 0.05 μm Al_2O_3 polishing powder and chamois, washed and placed in anhydrous ethanol for 1 min and placed in a dry dish for 1 d.

The IB used in this experiment was obtained from a bacteria bank of Huazhong University of Science and Technology. The IB medium used for separation and purification had the following composition: 0.5 g $MgSO_4$, 0.5 g $(NH_4)_2SO_4$, 0.5 g K_2HPO_4, 0.2 g $CaCl_2$, 0.5 g $NaNO_3$ and 10.0 g $C_6H_8FeNO_7$. After 14 days of incubation at 29 ± 1 °C, the conical flask with black or brown precipitation and red-brown color fading in the medium and becoming colorless and transparent or with this trend was judged to have iron bacteria. After taking it out and repeating the above steps to isolate and purify, the experimental bacteria were obtained after 3–4 generations of repeated culture.

The experimental water was prepared according to the quality specifications of the reclaimed water used as circulating cooling water.[20] Chemicals used in synthesizing the experimental water together with their respective concentrations are shown in Table 1. Three groups of tests were conducted: (1) the samples were in the conventional reclaimed water inoculated with IB, $1Cl_{IB}$; (2) the samples were in the reclaimed water with 3 times the Cl^- concentration inoculated with IB, $3Cl_{IB}$; (3) the samples were in the reclaimed water with 4 times the Cl^- concentration inoculated with IB, $4Cl_{IB}$. Table 2 shows the actual ion concentrations and the dosage of IB for each experimental condition.

2.2 Experimental devices

A combination of dynamic experiments and electrochemical tests were used. The dynamic test device, shown schematically in Fig. 1, is a self-built annular reactor with a volume of 2.5 L, the device simulates the hydraulic flow in the circulating cooling water pipe network. The temperature and rotational speed were set at 30 °C and 60 revs per min, respectively. The water pump supplied water to the device for each working condition every 2 hours. The experimental period was 15 days.

The corrosion weight loss, the number of IB on the surface of the coupons and the number of suspended IB in the water were measured and analyzed on 1st, 3rd, 7th, 11th, and 15th day of the experiments. XPS was used to analyze the corrosion products on the surface of the coupons on 3rd, 7th, 11th, and 15th day. The Cl^- concentration analysis on the surface of the coupons was carried out on the 15th day.

The electrochemical test adopted the traditional three-electrode systems, and the experimental period was set to 15

Table 1 Concentration of chemicals used in water distribution

	Num. of IB (CFU mL^{-1})	Cl^- (mg L^{-1})	SO_4^{2-} (mg L^{-1})	NH_4^+ (mg L^{-1})	HCO_3^- (mg L^{-1})	pH
$1Cl_{IB}$	10^5	118.2	122.2	1.9	199	7.9
$3Cl_{IB}$	10^5	369.3	122.2	1.9	199	7.9
$4Cl_{IB}$	10^5	501.6	122.2	1.9	199	7.9

Table 2 Experimental water ion concentration

	NaCl (mg L^{-1})	Na_2SO_4 (mg L^{-1})	$(NH_4)_2SO_4$ (mg L^{-1})	$NaHCO_3$ (mg L^{-1})
$1Cl_{IB}$	194.7	173.4	6.9	274
$3Cl_{IB}$	608.6	173.4	6.9	274
$4Cl_{IB}$	826.7	173.4	6.9	274

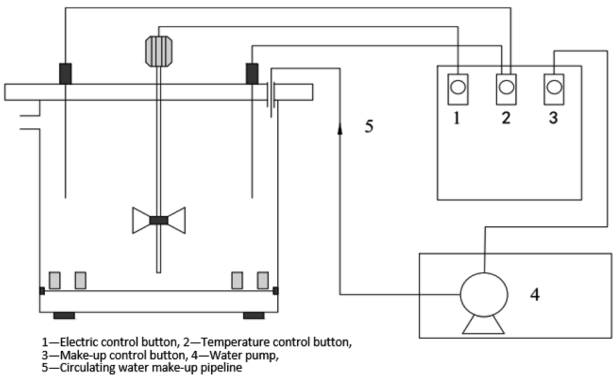

Fig. 1 Schematic diagram of dynamic reaction device.

days. On 1st, 3rd, 7th, 11th, and 15th day the polarization curve and electrochemical impedance spectroscopy (EIS) of different working conditions were measured.

2.3 Detection methods

The corrosion rate is calculated by the weight loss method, the calculation is as follows:

$$V = \frac{8760 \times 10 \times (m_1 - m_2)}{s \times t \times \rho} \quad (1)$$

where: V—corrosion rate, mm a^{-1}; m_1—the weight of the coupon before experiment, g; m_2—the weight of the coupon after experiment, g; ρ—the density of the coupon, 7.86 g cm^3; s—the surface area of the coupon, cm^2; t—running time, h; 8760, 10—calculation constants.

The variance is calculated from the triple sampling results and used as error bars for the test results.

The electrochemical workstation model was a CHI66C. The working electrode was a carbon steel electrode, the reference electrode was a saturated calomel electrode, and a platinum electrode was used as the auxiliary electrode. The polarization curve and EIS were measured for each working condition. For the determination of the polarization curve, the initial value of the open circuit potential should be set to −0.3 V, the termination value should be +0.3 V, and the scan rate should be adjusted to 1 mV s^{-1}. The polarization resistance was obtained from the same samples throughout the 15 day period. When measuring EIS, the initial level was set to the open circuit potential value, the high and low frequencies were adjusted to 100 000 and 0.01 Hz, and the amplitude was adjusted to 5 mV.

The carbon steel coupon was finally dried by a freeze dryer and the corrosion products scrapped off and ground into a powder. The composition of the corrosion products was analyzed using a PHI Quantera II X-ray photoelectron spectrometer. The XPS spectrum needed to be corrected by C 1s external standard method, and then the peak position on the test curve was analyzed by CASA software.

On 15th day, the carbon steel coupon was taken out, then dried on a filter paper. The corrosion layer was then scraped off and placed in a dry centrifuge tube. The corrosion products were then shaken in water in the centrifuge and left to settle, the supernatant was then recovered for later use. A HACH DR6000 UV spectrophotometer was used to measure the Cl^- concentration. The specific test method was carried out in accordance with the requirements of Hach Company's "Water Analysis Manual (Fifth Edition)".

The MPN technique was used to detect the number of IB suspended in water and on the surface of carbon steel coupons respectively. Five points at different depths and different positions in the reactor were selected to collect water samples which were then mixed uniformly. The water samples were diluted and inoculated with IB medium. After culturing at 29 ± 1 °C for 14 days, the count was taken out and counted as the number of suspended IB. The coupons were taken out at the same time of the day each time measurements were done, and the biofilm and corrosion products were scraped from the surface of the coupons and placed in a sterile sampling tube. The attached IB were incubated and counted using the same method. The research flow chart as shown in Fig. 2.

3 Results and discussion

3.1 Corrosion rate test

During the experiment, the average corrosion rate of carbon steel changed over time for all conditions as shown in Fig. 3.

According to Fig. 3, the corrosion rate for $4Cl_{IB}$ and $3Cl_{IB}$ on the 1st day was 1.47 and 1.27 times that of $1Cl_{IB}$ respectively. The results show that, in the initial stages of the experiment, the higher the Cl^- concentration, the faster the corrosion rate. However, as time progressed, a rapid decline in the corrosion rate for higher the Cl^- concentrations was observed while the corrosion rate for $1Cl_{IB}$ remained steadily increasing. After about the 9th day, the corrosion rates of $3Cl_{IB}$ and $4Cl_{IB}$ were lower than that of $1Cl_{IB}$. On the 15th day the corrosion rates of $3Cl_{IB}$ and $4Cl_{IB}$ were 7.0% and 15.6% lower than that of $1Cl_{IB}$. At the beginning of the experiment, the IB biofilm was immature, and the carbon steel interface was mainly covered by corrosion products. Bo's result have shown that higher Cl^- concentration dismantles the corrosion product layer and accelerates the corrosion of carbon steel.[21] This means that the higher the concentration of Cl^-, the more Fe^{2+} gets generated by corrosion.[22] The IB are known to oxidize Fe^{2+} in order to obtain the

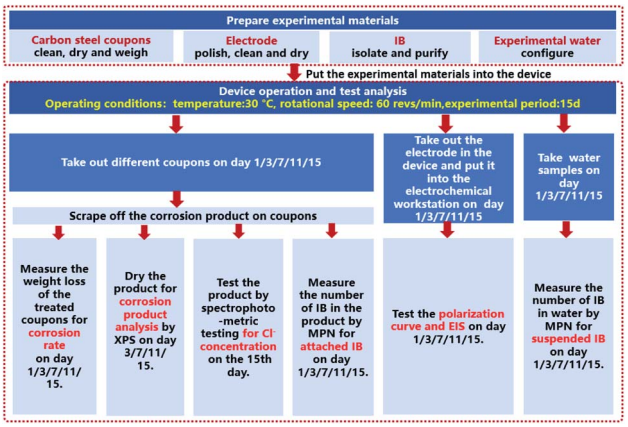

Fig. 2 Research flow chart.

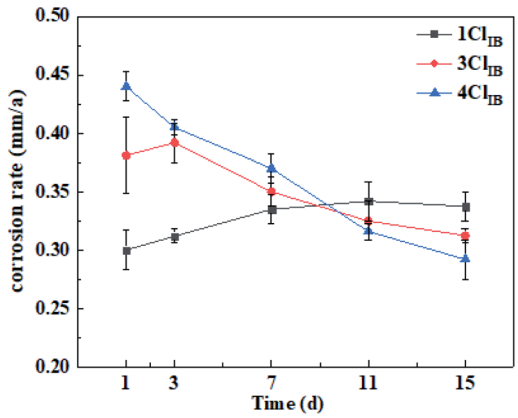

Fig. 3 The carbon steel corrosion rate in different Cl^- concentrations inoculated IB.

energy required to sustain their lives. The Fe^{3+} generated precipitate as iron(III) oxide that forms anodic active sites on the metal surface, promoting local corrosion.[23,24] However, in the later stages of corrosion, the results indicate that the higher the Cl^- concentration in the IB system reduces the corrosion rate. Qi's study found that in the absence of bacteria, the high Cl^- concentration promoted corrosion reaction over a period of 25 days,[25] which was not consistent with the results in this study which was conducted in the presence IB. The reason why a decline in the corrosion rate was observed in the later stages of corrosion might be due to the increasing thickness of biofilm formed by IB which captures and immobilizes corrosion products and inhibit corrosion. Studies have found that IB biofilms were conducive to the precipitation of corrosion products and together form a denser structure, which has a greater inhibitory effect than pure iron oxides.[26] In addition, the corrosion rate reached the peak in the earlier stages of corrosion for the higher the chloride ion concentration ($4Cl_{IB}$ & $3Cl_{IB}$) and reached a peak on the 11th day for the lower concentration ($1Cl_{IB}$), the peak values for $4Cl_{IB}$, $3Cl_{IB}$ and $1Cl_{IB}$ were 0.450, 0.392 and 0.342 mm a^{-1} respectively, which appeared 1st, 3rd and 11th day. It is suggested that the more severe corrosion reaction observed at the initial stage of corrosion for higher concentrations causes the rapid growth of the protective film resulting in the early onset corrosion inhibition.

3.2 Electrochemical measurements

3.2.1 Potentiodynamic polarization curve measurements. The potentiodynamic polarization curves of carbon steel electrodes immersed for 1–15 days are shown in Fig. 4. The parameters obtained by fitting the polarization curve are listed in Table 3. According to Table 3, the corrosion current density I_{corr} first increased and then decreased with time in all three working conditions. The corrosion potential E_{corr} first moved towards negative direction and then to positive direction. This shows that the corrosion rate first increased and then decreased with time.[27] On the 1st day, the I_{corr} value of the $1Cl_{IB}$ condition was the smallest, at 8.559 μA cm^{-2}, while that of $3Cl_{IB}$ and $4Cl_{IB}$ were 9.964 and 12.061 μA cm^{-2} respectively. The results clearly indicate that the high concentration of Cl^- made the corrosion reaction more severe at the beginning of corrosion process which is in agreement with the experimental results on corrosion rate measurements. The maximum current density for $1Cl_{IB}$, of 9.710 μA cm^{-2} was recorded on the 11th day while the maximum current densities for $3Cl_{IB}$ and $4Cl_{IB}$ of 11.165 and 12.584 μA cm^{-2} were recorded on the 7th and 3rd day. On the 15th day, the I_{corr} values of $4Cl_{IB}$ and $3Cl_{IB}$ were 14.2% and 6.9% lower than those of $1Cl_{IB}$, and both were lower than the values on the 1st day. This further demonstrates that high concentrations of Cl^- have an inhibitory effect on the corrosion

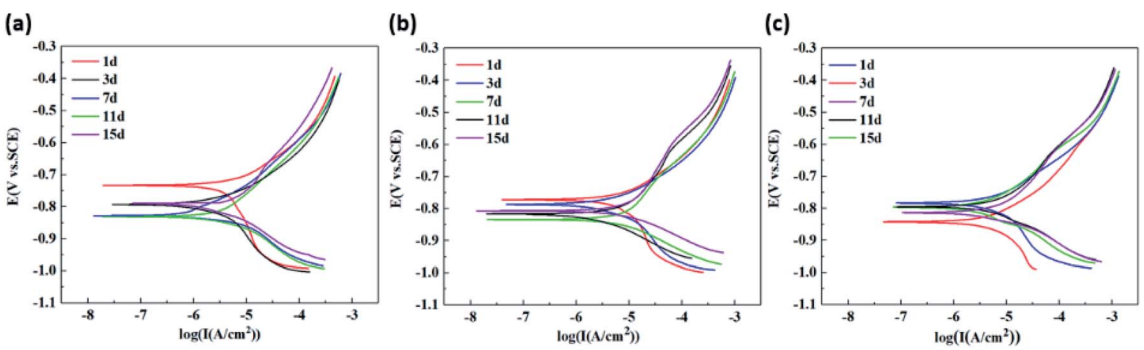

Fig. 4 The potentiodynamic polarization curves of carbon steel electrodes immersed for 1–15 days.

Table 3 Electrochemical parameters fitted from the potentiodynamic polarization curves

Time/d	β_a/mV	β_c/mV	I_{corr}/(μA cm^{-2})	E_{corr}/V
$1Cl_{IB}$				
1	166.82	238.35	8.559	−0.733
3	133.50	192.35	8.922	−0.793
7	130.27	147.71	9.522	−0.828
11	187.52	104.88	9.710	−0.831
15	202.83	136.47	9.634	−0.803
$3Cl_{IB}$				
1	129.13	240.46	9.964	−0.772
3	125.08	198.08	10.285	−0.787
7	124.55	82.63	11.165	−0.834
11	196.66	97.60	9.307	−0.816
15	198.28	107.28	8.969	−0.807
$4Cl_{IB}$				
1	110.39	244.87	12.061	−0.783
3	85.21	217.34	12.584	−0.842
7	148.05	93.48	10.357	−0.813
11	175.94	115.34	9.007	−0.795
15	191.03	128.32	8.268	−0.789

reaction in the later stage of corrosion in the presence of IB. The effect of Cl^- concentration was consistent with what was observed from the corrosion rate measurements and the I_{corr} peaks were also consistent with the time sequence in which the corrosion rate peaks were observed.

The anodic reaction on the surface of carbon steel is the dissolution of carbon steel, and the cathodic reaction is the reduction of oxygen. According to Table 3, the β_a and β_c of the three working conditions showed a similar trend of the values first decreasing and then increasing. It shows that the corrosion reaction in the early stage is gradually intensified, and the corrosion products in the later stage are gradually accumulated, which hinders the continuation of the cathodic and anode reactions. The results are consistent with the corrosion rate, I_{corr} and E_{corr}.

At the same time, on the 1st day, the absolute value of the cathodic Tafel slope of the polarization curves (β_c) for three working conditions were higher the value of the anodic Tafel slope of the polarization curves (β_a), and they were in the range of 238.35–244.87 mV. Cathodic reactions are shown to be the controlling factor of corrosion at this time. However, with the extension of time, the increase of β_a values was larger. By the 15th day, the β_c values of the $1Cl_{IB}$, $3Cl_{IB}$ and $4Cl_{IB}$ conditions were 0.6, 0.5 and 0.5 times higher than those of the 1st day, while the β_a values were 1.2, 1.5 and 1.7 times higher than those of the 1st day. At this stage, the anode reaction becomes the controlling factor of corrosion process, and the higher the Cl^- concentration, the greater the confinement effect of the anode. Therefore, it can be inferred that the reduction of the corrosion reaction rate in the later stages of the corrosion process is due to the inhibition of anodic iron dissolution reaction. This is most likely due to the hindering effect of the IB biofilm and corrosion product layer. In the later stages, the β_c of the three working conditions all increased slightly, indicating that the dissolved oxygen mass transfer was also affected by the biofilm and corrosion product layers.

Comparison of β_a values at the same time show that the values for $3Cl_{IB}$ and $4Cl_{IB}$ conditions were 22.6% and 33.8% lower than those for $1Cl_{IB}$ condition, which indicates that the higher the Cl^- concentration at this stage, the easier it is for the anode to lose electrons.[28] Jiang and Li also found that the erosive effect of Cl^- and the metabolism of IB promoted the anodic reaction.[29,30]

3.2.2 EIS analysis. The Nyquist plots of carbon steel electrodes immersed for 1–15 days are shown in Fig. 5. On the 1st day, the order of semicircle diameters of the Nyquist plots from small to large was $4Cl_{IB} < 3Cl_{IB} < 1Cl_{IB}$. In 3–7 days, their gap was narrowed. On 11th day, the order became $1Cl_{IB} < 3Cl_{IB} < 4Cl_{IB}$. In general, the larger the diameter of the Nyquist semicircle, the lower the corrosion rate.[31] The experimental results suggest that in the early stages, the higher the Cl^- concentration, the smaller the impedance, so the corrosion reaction was accelerated at higher Cl^- concentrations.[32]

However, over time, the corrosion rate slowed down suggesting that on the contrary, the high concentration of Cl^- increased the impedance and inhibited the corrosion reaction. The results were consistent with the observations made in both the corrosion rate and polarization curves.

ZSimpWin software was used to fit the circuit. The equivalent circuit is shown in Fig. 6, and the fitted parameters are shown in Table 4. The meanings of the relevant parameters in Fig. 5 and Table 4 are as follows:[33] R_s represents the solution resistance, R_{ct} is the charge transfer resistance at the interface, R_b and Q_b represent the film resistance and capacitance formed by the corrosion product layer and biofilm, and double layer capacitance are described by Q_{dl}, n_b and n_{dl} are the dispersion index. The χ^2 test indicates the fitting effect, and the χ^2 values of ideal circuits are generally considered to be in the range of 10^{-3} to 10^{-5},[34] and the χ^2 values of all data in this study were within the required range.

According to Fig. 5 and Table 4, although the fitted circuits conform to the R(Q(R(QR))) model for all three operating, there are large differences in the variation of their R_b and R_{ct} values with increasing time. On the 1st day, the R_b of $1Cl_{IB}$, $3Cl_{IB}$ and $4Cl_{IB}$ were only in the range 13.8–42.1 Ω cm^2, all much smaller than the R_{ct} values of 1249–1848 Ω cm^2, demonstrating that the impedance in all three conditions at this time were chiefly from the interfacial charge transfer resistance, and the effect of film resistance was minimal. Moreover, the high Cl^- concentration condition exhibited lower R_{ct} values. However, thereafter, R_b kept reducing and R_{ct} kept decreasing, and the higher the Cl^- concentration, the greater the variation. On the 15th day, the R_{ct} of the $4Cl_{IB}$ condition was 39.8% and 12.4% lower than the R_{ct} of $1Cl_{IB}$ and $3Cl_{IB}$, but the R_b was 2.60 and 0.83 times higher. The R_b was 1592.1 Ω cm^2, which was 1.9 times higher than the R_{ct}. It means that at this time, the impedance primarily comes concentration, the faster and denser the biofilm and corrosion product layer were formed, and therefore, the less likely corrosion would occur. It proves that the hypothesis of this study on the cause of corrosion rate decrease was sound. Both Ghafari *et al.*[35] and Scheerder *et al.*[36] found that the carboxyl groups of

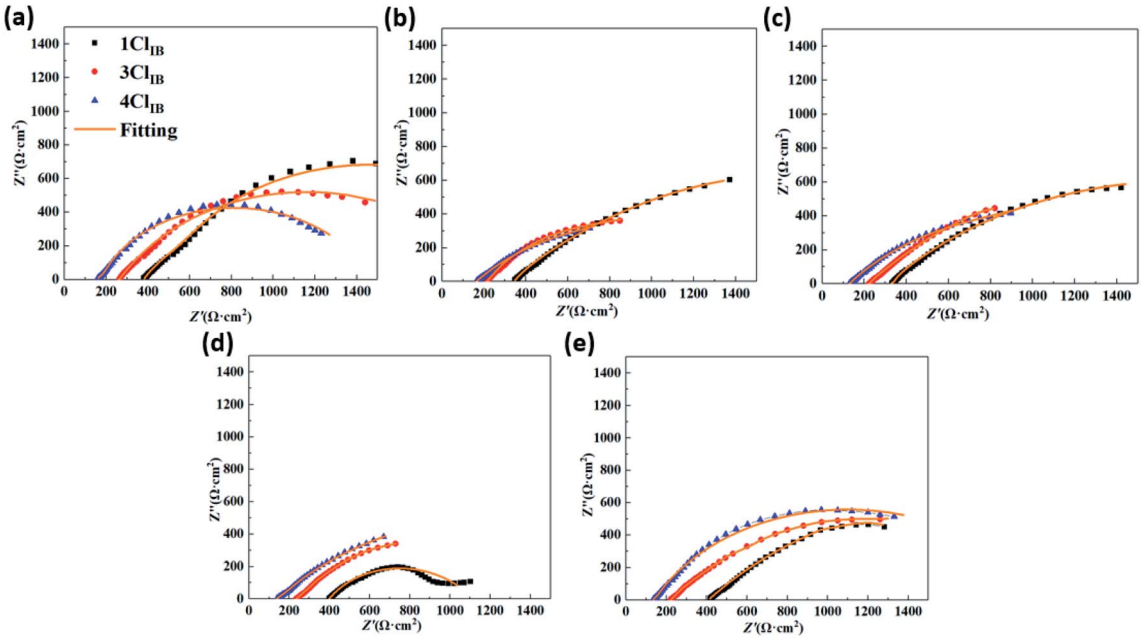

Fig. 5 Nyquist diagram of carbon steel electrode: (a) 1 d; (b) 3 d; (c) 7 d; (d) 11 d; (e) 15 d.

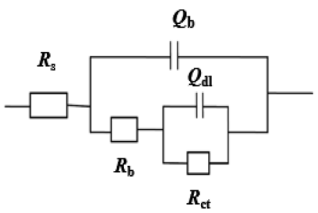

Fig. 6 Fits the equivalent circuit diagram.

polysaccharides in extracellular polymers (EPS) secreted by IB contain C–O and C=O bonds that can complex with Fe(II/III) and are responsible for the formation of a denser shielding layer.

3.3 Corrosion product analysis

In order to evaluate the formation and transformation process of corrosion products under the different experimental conditions, the composition was analyzed semi-quantitatively using XPS technique. The Fe 2p spectra were fitted to the split peaks using CASA software. And Fig. 7 shows the results of the proportion of iron oxide content extracted based on the fitting results. The corrosion products initially consisted of FeOOH, Fe_2O_3, and later Fe_3O_4.

As can be seen from Fig. 7, the corrosion products formed at different experimental conditions were of three distinct crystal types which are FeOOH, Fe_2O_3 and Fe_3O_4. The conversion of the

Table 4 The electrochemical impedance parameters obtained by fitting the circuit

Time (d)	Q_b (μF cm^{-2})	n_b	R_b (Ω cm^2)	Q_{dl} (μF cm^{-2})	n_{dl}	R_{ct} (Ω cm^2)
1Cl$_{IB}$						
1	812	0.63	13.8	495	0.76	1848
3	1254	0.68	19.7	1100	0.67	1815
7	1907	0.71	63.8	2108	0.51	1627
11	1985	0.81	176.8	3189	0.60	1496
15	2757	0.94	442.0	10 550	0.61	1388
3Cl$_{IB}$						
1	0.678	0.99	20.9	1067	0.67	1499
3	1.89	1.00	169.2	2372	0.62	1340
7	3599	0.63	383.1	2432	0.51	1258
11	5811	0.56	560.3	1136	0.80	1197
15	7415	0.57	869.0	580	0.89	954
4Cl$_{IB}$						
1	2.98	1.00	42.1	171	0.61	1249
3	1119	0.69	280.5	194	0.56	1128
7	2601	0.62	530.4	2776	0.54	1033
11	3680	0.54	842.0	883	1.00	973
15	4484	0.51	1592.1	591	1.00	836

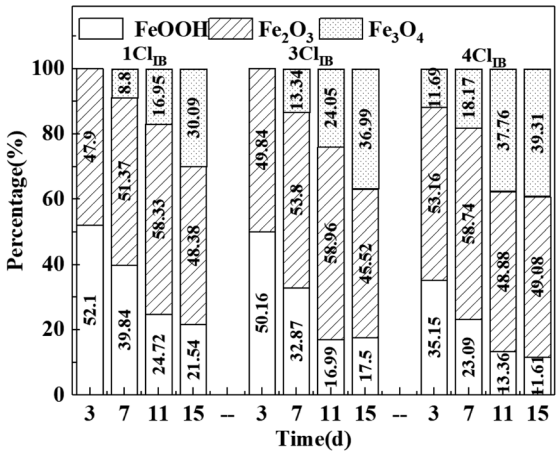

Fig. 7 XPS results of iron oxide composition on carbon steel surface.

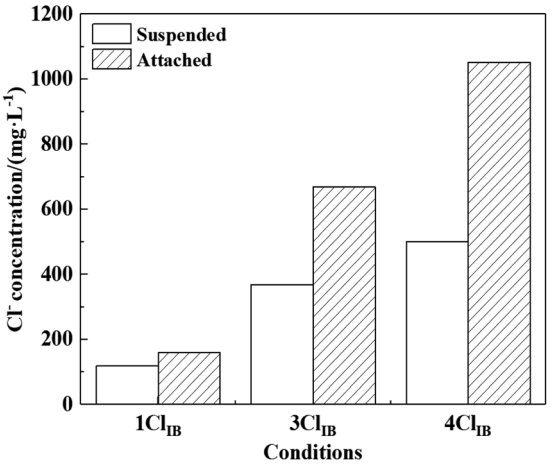

Fig. 8 Cl^- concentration in biofilm on 15th day.

unstable FeOOH to the more stable Fe_2O_3 and Fe_3O_4 occurred with increasing reaction time. Fe_3O_4 was detected on 3rd day for $4Cl_{IB}$ whilst it was detected on 7th day for $1Cl_{IB}$ and $3Cl_{IB}$. The percentage of FeOOH was the lowest and the percentage of Fe_3O_4 was the highest in all $4Cl_{IB}$ conditions during the experiment. In comparison with $1Cl_{IB}$ and $3Cl_{IB}$ conditions, the percentage of Fe_3O_4 in $4Cl_{IB}$ was 9.22% and 2.32% higher on 15th day. The reason for this observation might be that the elevated Cl^- concentration at the beginning of corrosion caused a high corrosion rate, that resulted in the anode surface accumulating too much $Fe(OH)_2$ and Fe^{2+}, promoting the conversion of corrosion products to Fe_3O_4.[37] It was also likely that simultaneously the IOB metabolism rapidly consumed dissolved oxygen, creating an anaerobic environment for IRB bacteria whose metabolic activity also produced Fe_3O_4.[38] The results of corrosion product analysis reveal that the high concentration of Cl^- accelerates the conversion of the unstable corrosion product FeOOH to the stable product Fe_3O_4 in the IB system, making the corrosion product layer denser. This is consistent with the analysis of the cause of the rapid rise in film resistance in EIS, verifying the paper's conjecture of the cause of the corrosion rate decline.

3.4 Cl^- concentration detection

Corrosive ions impact the growth and attachment of IB, while the erosion of carbon steel by corrosive ions is also influenced by the growth of IB, especially their biofilm. The Cl^- concentration on the carbon steel surface was measured on 15th day under different working conditions, and the results are shown in Fig. 8. The enrichment effect was evident after the increase of Cl^- concentration, in which the Cl^- concentration inside the biofilm was 1.81 times and 2.10 times higher than that in water under $3Cl_{IB}$ and $4Cl_{IB}$ conditions respectively. In the presence of high concentration of Cl^- and IB, iron oxides precipitation increased, which lead to more pronounced adsorption.[39,40]

In addition, both IRB and higher Cl^- concentration stimulate the production of green rust, which allows a sustained flow of inorganic ions from the solution into the biofilm.[41]

The anodic reaction of metallic iron corrosion was originally reaction (2), but Darwish *et al.*[42] and Burstein *et al.*[43] found that Cl^- can facilitate the dissolution of anodic iron by catalytic reaction (reactions (3)–(5)), which makes the corrosion reaction accelerate. In the late stage of corrosion, the protective film became the controlling factor of the corrosion reaction, preventing reactions (2)–(5) from occurring. The above demonstrates that high concentration of Cl^- makes the corrosion product layer denser, and the effect of Cl^- on biofilms will be further discussed in detail in 3.5.

$$Fe \rightarrow Fe^{2+} + 2e^- \quad (2)$$

$$Fe + Cl^- + H_2O \rightarrow [FeCl(OH)]_{ad}^- + H^+ + e^- \quad (3)$$

$$[FeCl(OH)]_{ad}^- \rightarrow FeClOH + e^- \quad (4)$$

$$FeClOH + H^+ = Fe^{2+} + Cl^- + H_2O \quad (5)$$

3.5 IB characteristics analysis

The trend of the number of IB in different working conditions is shown in Fig. 9. The number of suspended IB in $4Cl_{IB}$ on 1st day was 50 and 17 times higher than that of $1Cl_{IB}$ and $3Cl_{IB}$, respectively. It indicates that high concentration of Cl^- can promote the growth of suspended IB. Subsequently, the number

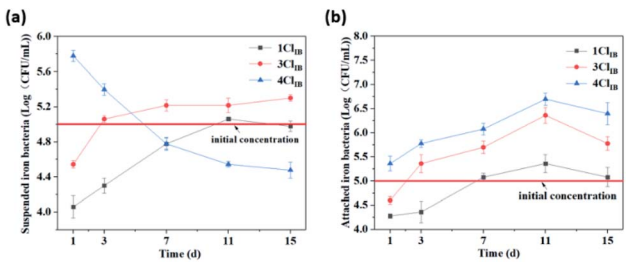

Fig. 9 The number of IB, (a) suspended; (b) attached.

of suspended IB in $1Cl_{IB}$ and $3Cl_{IB}$ both increased with time, but that for $4Cl_{IB}$ showed a decrease. The number of IB attached to the carbon steel interface within 15 days is shown in Fig. 9(b). Compared to the $1Cl_{IB}$ and $3Cl_{IB}$ conditions, the $4Cl_{IB}$ had an average of 1–1.5 orders of magnitude higher levels of attached IB. In comparison with the test results of Cl^- concentration at the interface, the Cl^- content at the interface of $4Cl_{IB}$ was 6.58 and 1.57 times higher than that of $1Cl_{IB}$ and $3Cl_{IB}$ on 15th day, which indicates that the high concentration of Cl^- promoted the adhesion of IB on the surface of carbon steel. Initially, the high Cl^- concentration, which released more Fe^{2+}, led to faster growth of IB and faster biofilm formation. This resulted in less Fe^{2+} released into the water, leading to less IB in the water, but the number of IB in the biofilm continued to rise because of easier access to Fe^{2+}.

The optimum concentration of Cl^- to promote the growth of IB was not established during the experiment. It may be due to the fact that this promotion is not mainly achieved by salt elevation, but because IB can oxidize the Fe^{2+} precipitated by corrosion to Fe^{3+} and derive energy from it,[44,45] while this process also promotes the corrosion reaction to occur.

As time progressed, the increased Cl^- concentration promoted the formation of IB biofilms, which, together with the dense corrosion products, formed a structurally dense protective film under the action of EPS, hindering corrosion occurrence. The synergistic slowing of corrosion by biofilm and corrosion products was also observed in the study by Wang *et al.*[26] The experimental results of the IB characteristics analysis further prove the previous conjecture.

4 Conclusions

In this study, the effect of corrosive Cl^- ions on the corrosion behavior of carbon steel in IB system was investigated in the context of reclaimed water reuse for circulating cooling water. It was found that the corrosion reaction was promoted by the increase of Cl^- concentration in the early stage of corrosion, while with the extension of time, the high concentration of Cl^- slowed down the corrosion rate instead.

The increase in Cl^- concentration, on one hand, leads to the enrichment of Cl^- on the surface of carbon steel and in the corrosion product layer, which destroys the passivation film and increases the dissolved Fe^{2+}. At the same time IB metabolic operations were also increased. Both of these make the anode potential and charge transfer resistance drop, accelerating the corrosion process. During this period, the anodic reaction may have been accelerated by the catalytic effect of Cl^- and iron bacterial metabolism, and the iron solubilization reaction was accelerated. The rapid corrosion reaction results in a rapid accumulation of corrosion products and rapid consumption of dissolved oxygen. On the other hand, increased concentration of Fe^{2+} and oxygen starvation providing conditions for IRB to survive, this results in an increase of more dense corrosion products Fe_3O_4. Meanwhile, with the development of time, the higher the concentration of Cl^-, which causes the higher number of attached IB in the system result in the faster development of the denser biofilm. The EPS secreted by IB can complex with corrosion products, forming a denser protective film and inhibiting the anodic Fe^{2+} leaching. The experimental results showed a significant increase in anode slope and membrane impedance. At the same time, the cathodic slope also increased, indicating that the reduction reaction of oxygen was also affected. In summary, high concentration of Cl^- exhibits corrosion-inhibiting effect in the later stage of corrosion.

To further investigate the effect of chloride ions on growth factors affecting iron bacterial corrosion. Further studies are needed to clarify the mechanism of Cl^- effects on metabolic behavior, biofilm structure, and adhesion behavior of iron bacteria.

Conflicts of interest

There are no conflicts to declare.

Acknowledgements

This study was supported by the National Natural Science Foundation of China (No. 51578035).

Notes and references

1 S. J. Cai, X. Y. Zhao and Y. Y. Wang, *Ind. Water Treat.*, 2009, **29**, 4.
2 J. Jin, G. Wu and Y. Guan, *Water Res.*, 2015, **17**, 207.
3 X. Xu, S. Liu, K. Smith, Y. Cui and Z. Wang, *J. Clean. Prod.*, 2020, **276**(10), 124079.
4 Z. Panossian, N. Almeida, R. Sousa, G. Pimenta and L. Marques, *Corros. Sci.*, 2012, **58**, 1.
5 B. Hou, X. Li, X. Ma, C. Du, D. Zhang, M. Zheng, W. Xu, D. Lu and F. Ma, *npj Mater. Degrad.*, 2017, **1**, 4.
6 H. Liu, C. Fu, T. Gu, G. Zhang, Y. Lv, H. Wang and H. Liu, *Corros. Sci.*, 2015, **100**, 484.
7 Y. Tang, Z. Yu, J. Wang, X. Zhao, B. Niu and L. Bing, *Corros. Sci.*, 2014, **80**, 111.
8 H. Li, C. Dong, K. Xiao, X. Li and P. Zhong, *Int. J. Miner., Metall. Mater.*, 2016, **23**, 1286.
9 Y. An, *The study of localized corrosion mechanism of typical engineering metal material in seawater containing microorganism*, Institute of Oceanology, Chinese Academy of Science, Qingdao, Doctoral Dissertation, 2010, p. 18.
10 H. X. Li, D. P. Li, L. Zhang, Y. W. Wang, X. Y. Wang and M. X. Lu, *Int. J. Miner., Metall. Mater.*, 2019, **26**, 329.
11 H. Wang, L. Ju, H. Castaneda, C. Gang and B. Newby, *Corros. Sci.*, 2014, **89**, 250.
12 S. Chen, The study of localized corrosion mechanism of typical engineering metal material in seawater containing microorganism, Doctoral Dissertation, *Institute of Oceanology, Chinese Academy of Science, Qingdao*, 2015, **vol. 109**.
13 J. Starosvetsky, R. Kamari, Y. Farber, D. Bilanovic and R. Armon, *Corros. Sci.*, 2016, **102**, 446.
14 H. Wang, C. Hu, L. Zhang, X. Li and Y. Min, *Water Res.*, 2014, **65**, 362.

15 Z. Li, J. Wang, Y. Dong, D. Xu and F. Wang, *J. Mater. Sci. Technol.*, 2021, **71**, 177.
16 T. I. Wu and J. K. Wu, *Corrosion*, 1995, **51**, 185.
17 Y. H. Wang, Q. Wang, S. R. Yu and Y. L. Song, *J. South China Univ. Technol., Nat. Sci.*, 2008, **36**, 92.
18 Z. Zin, Y. Yu, Y. C. Wang, P. Q. Zhang, J. Z. Duan and B. R. Hou, *Corros. Prot.*, 2014, **47**, 57.
19 S. F. Zhou, X. F. Yin, W. G. Zhou, C. Sun and A. H. Han, *Corros. Sci. Prot. Technol.*, 2004, **16**, 4.
20 Y. Chu, P. Xu, Y. Ou, P. Bai and Z. Wei, *Sci. Total Environ.*, 2020, **718**, 136679.
21 S. C. Bo, China University of Petroleum, Qingdao, 2010, **41**.
22 J. L. Gao, *Research of influencing factors on iron release in water distribution system*, Zhejiang University, Hangzhou, 2013, p. 23.
23 H. Wang, C. Hu and X. Li, *Eng. Failure Anal.*, 2015, **57**, 423.
24 C. G. E. M. V. Beek, T. Hiemstra, B. Hofs, M. M. Nederlof, J. A. M. V. Paassen and G. K. Reijnen, *Aqua*, 2012, **61**, 1.
25 Y. Qi, *The study of influence caused by water quality factors on stainless steel material in reclaimed water and corrosion control*, Beijing Jiaotong University, Beijing, 2017, 38.
26 H. B. Wang, C. Hu, X. X. Hu, M. Yang and J. H. Qu, *Water Res.*, 2012, **46**, 1070.
27 H. Qian, J. Zhang, T. Cui, L. Fan, X. Chen, W. Liu, W. Chang, C. Du and D. Zhang, *Bioelectrochemistry*, 2021, **140**, 107746.
28 K. Pranav, S. S. Su, M. S. Mannan, H. Castaneda and S. A. Vaddiraju, *Ind. Eng. Chem. Res.*, 2018, **57**, 13895.
29 Z. G. Jiang, H. H. Wang, L. H. Gong, G. P. Chen and X. J. Chen, *Mater. Prot.*, 2017, **50**, 74.
30 S. H. Li, Y. Y. Zhang, J. H. Liu and M. Yu, *Acta Phys.-Chim. Sin.*, 2008, **24**, 1553.
31 S. J. Yuan, A. M. F. Choong and S. O. Pehkonen, *Corros. Sci.*, 2007, **49**, 4352.
32 M. Zhu, C. W. Du, X. G. Li, Z. Y. Liu, S. R. Wang, T. L. Zhao and J. H. Jia, *J. Mater. Eng. Perform.*, 2014, **23**, 1358.
33 H. Liu and Y. F. Cheng, *Electrochim. Acta*, 2018, **10**, 312.
34 M. Behpour, S. Ghoreishi, N. Mohammadi, B. N. Soltani and N. M. A. Salavati, *Corros. Sci.*, 2010, **52**, 4046.
35 M. Ghafari, A. Bahrami, I. Rasooli, D. Arabian and F. Ghafari, *Int. Biodeterior. Biodegrad.*, 2013, **80**, 29.
36 J. Scheerder, R. Breur, T. Slaghek, W. Holtman, M. Vennik and G. Ferrari, *Prog. Org. Coat.*, 2012, **75**, 224.
37 M. Yamashita, H. Miyuki, Y. Matsuda, G. Nagano and T. Misawa, *Corros. Sci.*, 1994, **25**, 283.
38 H. F. Sun, B. Y. Shi, D. A. Lytle, Y. H. Bai and D. S. Wang, *Environ. Sci.: Processes Impacts*, 2014, **16**, 576.
39 A. Jaiswal, S. Banerjee, M. Raj and M. C. Chattopadhyaya, *J. Environ. Eng.*, 2013, **1**, 281.
40 K. Jafarzadeh, S. Shahrabi and M. M. Hadavi, *J. Mater. Sci. Technol.*, 2007, **5**, 623.
41 J. T. Jin, *The biological-chemical coupling mechanism of microbiallly influenced corrosion in reclaimed wastewater pipeline*, Tsinghua University, Beijing, 2015, p. 11.
42 N. A. Darwish, A. Hilbert, W. J. Lorenz and H. Rosswag, *Electrochim. Acta*, 1973, **18**, 421.
43 G. T. Burstein and D. H. Davies, *Corros. Sci.*, 1980, **20**, 28.
44 S. C. Neubauer, D. Emerson and J. P. Megonigal, *Appl. Environ. Microbiol.*, 2002, **68**, 3988.
45 E. E. Roden, D. Sobolev, B. Glazer and G. W. Luther, *Geomicrobiol. J.*, 2004, **21**, 379.